Journal of Catalysis **184,** 59–67 (1999)
Article ID jcat.1999.2451, available online at http://www.idealibrary.com on IDEAL®

The Role of Titania Support in Mo-Based Hydrodesulfurization Catalysts

Jorge Ramirez,* Luis Cedeño,* and Guido Busca†

*UNICAT, Departamento de Ingeniería Química, Facultad de Química, UNAM, México D.F. (04510), México; and †Istituto di Chimica, Facoltá di Ingegneria, Universita di Genova, P. le J.F. Kennedy, I-16129 Genova, Italy
E-mail: jrs@servidor.unam.mx

Received June 26, 1998; revised February 10, 1999; accepted February 11, 1999

A series of mechanical mixtures Mo/Al_2O_3–TiO_2/Al_2O_3 has been prepared to study the role of titania in Mo-based HDS catalysts. The catalysts were tested in the thiophene hydrodesulfurization reaction at atmospheric pressure and were characterized by UV–vis diffuse reflectance spectroscopy (DRS), TPR-S (after reaction), and high-resolution electron microscopy (HREM). The results show that the titanium species formed during sulfidation and HDS reaction act as promoter of the Mo phase giving rise to a synergy effect. This synergy effect seems to be related to the electronic properties of the partially reduced and/or sulfided TiO_2 surface and, in particular, to the presence of Ti^{3+} ions. Finally, estimation of the number of sulfur vacancies created on the used catalysts during TPR-S indicate that only a small proportion of all the edge/corner Mo atoms present in the MoS_2 crystallites, estimated from HREM observations, are active in HDS and that a low number of sulfur vacancies are required.

Key Words: **Mo HDS catalysts; titania role.**

INTRODUCTION

The need for better hydrodesulfurization catalysts to comply with increasingly strict environmental regulations has promoted research on the use of new supports and active phases to improve the performance of hydrodesulfurization catalysts. Among the new supports, titania (1–3) and alumina–titania mixed oxides (4, 5) have shown promising results. It has been found that for thiophene hydrodesulfurization, Mo catalysts supported on titania are 4.4 times more active that those supported on alumina (1). Similar behavior has also been observed for tungsten-based catalysts (6). Another interesting observation is that the synergetic effect of the cobalt promoter in CoMo HDS catalysts is greater for the catalysts supported on alumina than for those supported on titania (1), despite that the catalytic activity of the CoMo catalysts supported on TiO_2 is 1.88 times higher than that of the one supported in Al_2O_3. Therefore, the main beneficial effect of the TiO_2 support appears to be on the Mo phases rather than on the Co promoter.

In the idea of taking advantage of the high activity of titania-supported Mo catalysts and of the excellent textural mechanical and thermal properties of alumina, catalysts supported on Al_2O_3–TiO_2 mixed oxides have also been proposed as HDS catalytic supports (7–9). However, when Al_2O_3–TiO_2 mixed oxides are used as supports for Mo- or W-based catalysts, at low titania loading the HDS activity per square meter of catalyst remains close to that of an alumina supported catalyst with similar metal loading, and significant activity increase is only observed for the catalysts supported on titania-rich Al_2O_3–TiO_2 mixed oxide supports (4), on which TiO_2 particles are present on the catalyst surface. The explanation to this behavior has been found in the fact that at titanium contents lower than a molar ratio $TiO_2/(Al_2O_3 + TiO_2) = 0.9$, the surface of the sol–gel prepared Al_2O_3–TiO_2 support is preferentially covered with alumina (10). However, despite all the previous studies, an explanation for the substantial difference in HDS activity between alumina- and titania-supported catalysts has not yet been elucidated, since the increase in activity when using TiO_2 as support cannot be completely explained by differences in dispersion or sulfidation of the active metallic species (1, 2). It is proposed here that to explain the previous activity results, the titania particles present on the surface of the support have to play an active role in the HDS reaction mechanism.

It is the object of the present work to analyze if the titania present in the support acts as a promoter, and if it is capable of creating a synergetic effect with the molybdenum sulfided phases, even when there is not an intimate physical contact between the Ti and Mo species. To this end, a series of mechanical mixtures, constituted by different amounts of Mo/Al_2O_3 and TiO_2/Al_2O_3, were tested in the thiophene HDS reaction and characterized in their sulfided state by temperature programmed reduction (TPRS) after reaction, high-resolution electron microscopy (HREM), and diffuse reflectance spectroscopy (DRS).

METHODS

Mechanical mixtures with various Mo/Al_2O_3–TiO_2/Al_2O_3 weight ratios ($MM = (Mo/Al_2O_3/(Mo/Al_2O_3 + TiO_2/Al_2O_3)) \times 100 = 0$, 20, 50, 80, 90, and 100%) were prepared from appropriate amounts of each previously calcined

0021-9517/99 $30.00

sample. The physical mixing was performed by fluidizing with dry air the mixture Mo/Al_2O_3–TiO_2/Al_2O_3 for 1 h. The Mo/Al_2O_3 catalyst was prepared by the pore–volume impregnation of a commercial γ-alumina support (Girdler, surface area 180 m^2/g), with an aqueous solution of ammonium heptamolybdate with the appropriate concentration to obtain 2.8 atoms of Mo/nm^2. After impregnation the catalyst was dried at 383 K for 24 h, followed by calcination at 773 K for 4 h. The titania-covered alumina (TiO_2/Al_2O_3) was prepared by impregnating the alumina support with an adequate amount of Ti–isopropoxide to obtain 11 wt% of TiO_2 and then, to achieve uniform hydrolysis, the solid sample was fluidized with an air stream saturated with water at room temperature for 24 h. The sample was then dried at 383 K for 12 h and finally calcined in air at 773 K for 4 h.

Before the catalytic test, the samples were sulfided at 673 K for 4 h using a stream of H_2S–H_2 (15% H_2S v/v). The catalytic activity tests for thiophene HDS were carried out at atmospheric pressure in a typical continuous differential micro-reactor apparatus. Briefly, hydrogen was bubbled through a saturator filled with thiophene and maintained at 275 K. The gas mixture was passed through a Pyrex glass reactor with temperature regulation. All the activity tests were made with the same total amount of catalyst (0.25 g), but the relative amounts of Mo/Al_2O_3 and TiO_2/Al_2O_3 in the mechanical mixture were varied. Reactant and product analysis was performed with a gas chromatograph equipped with a FID detector and an Ultra-I 30 m column.

For the TPR-S experiments the catalyst samples were cooled to room temperature immediately after the reaction, under a flow of nitrogen and transferred, also in a nitrogen atmosphere, to the TPR-S apparatus. TPR-S was performed in a flow apparatus using an argon–hydrogen (30% H_2 v/v) mixture as reducing gas and a thermal conductivity detector (TCD). The gas mixture flow was kept at 25 ml/min and the heating rate of the samples was 10 K/min. To measure the H_2S evolution a Perkin–Elmer 552 UV spectrophotometer set 200 nm and equipped with a flow cell was used. The spectrophotometer was operated in the absorption mode and was calibrated with H_2S–H_2 mixtures of different concentrations. It was found that at the usual concentrations of the experiment, the UV signal was directly proportional to the H_2S concentration.

The HREM micrographs of the sulfided catalysts were obtained on a Jeol 2010 microscope with a line resolution of 0.14 nm. UV–vis diffuse reflectance spectra (DRS) of the catalysts in the wavelength 250–2500 nm were obtained in a Cary 5E UV–vis–NIR spectrophotometer, using $BaSO_4$ as reference.

RESULTS AND DISCUSSION

The catalytic activities of the single Mo/Al_2O_3 and TiO_2/Al_2O_3 samples and of the different mechanical mixtures of these two systems were evaluated in the thiophene HDS reaction. Figure 1 shows the rate of reaction, expressed as molecules of thiophene converted per second and per nm^2, obtained at different temperatures with the Mo/Al_2O_3 and TiO_2/Al_2O_3 catalysts and with their mechanical mixtures. In this type of plot, if the catalyst behavior was that of a simple noninteracting mechanical mixture, one would expect the activity trend to be the proportional sum of the individual activities of Mo/Al_2O_3 and TiO_2/Al_2O_3. The first interesting observation that is not so evident in Fig. 1 due to the scale size in the ordinate axis was that, although small, the TiO_2/Al_2O_3 catalyst exhibited some activity in the thiophene HDS reaction (i.e., 4.98×10^{-6} molecule nm^{-2} s^{-1} at 593 K). The second interesting feature was that the observed rate for the mechanical mixtures was greater than that expected from the corresponding individual contributions of the components of the mechanical mixture, showing therefore the existence of a synergy effect due to the presence of TiO_2.

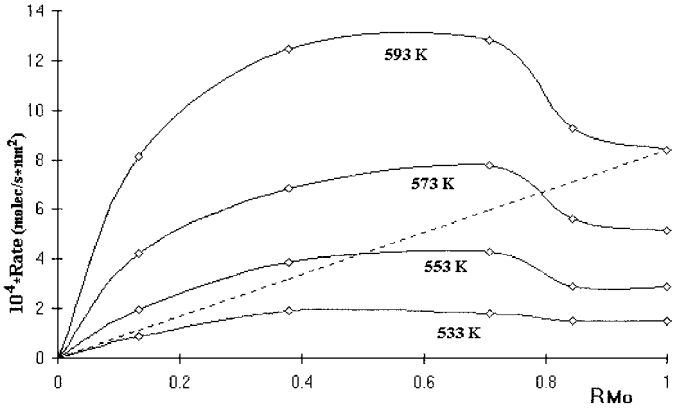

FIG. 1. Thiophene HDS reaction rate versus catalyst composition. $P = 1$ atm and several reaction temperatures. $R_{Mo} = (Mo/Ti + Mo)$ atomic ratio.

The magnitude of the synergy was calculated as the observed rate of reaction of the mechanical mixture divided by the rate of reaction expected from the proportional individual contributions of Mo/Al_2O_3 and TiO_2/Al_2O_3 (dotted line in Fig. 1). The results from this calculation, at four reaction temperatures, are presented in Fig. 2. It is clear from this figure that the synergy effect in the mechanical mixtures increases with titanium loading and also with reaction temperature. Clearly, the surface titanium species, which are at least partially reduced or sulfided, as we have shown previously (6), act as a promoter of the Mo/Al_2O_3 catalyst in the HDS reaction.

The fact that the titanium phases produce a synergy effect with the Mo-sulfided phase explains why previous published results show that incorporation of titania to the catalyst alumina support leads to greater activities than those expected from the observed changes in dispersion of the molybdenum sulfided species (4). However, why this

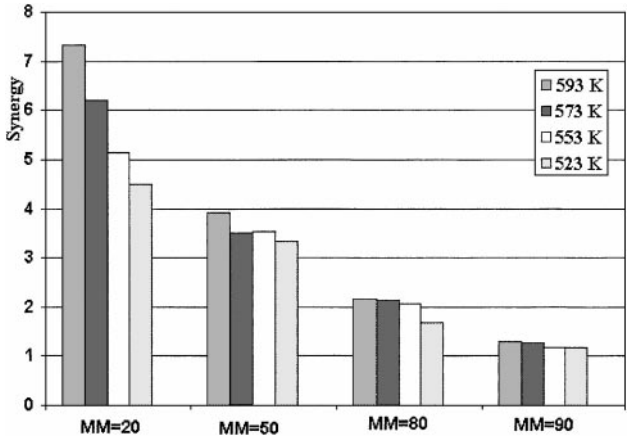

FIG. 2. Synergy effect of mechanical mixtures, evaluated as the observed rate of HDS reaction divided by the rate of reaction expected from the individual contributions of Mo/Al_2O_3 and TiO_2/Al_2O_3. Thiophene HDS reaction at $P = 1$ atm and several reaction temperatures.

happens is not so clear yet. In what follows we will try to go deeper into this question.

The changes induced by the presence of titania, on the molybdenum sulfided phases after the reaction test, can be assessed in part by the TPR-S technique. By means of this technique it is possible to follow the reduction of the molybdenum and titanium sulfide phases. Also, the amount of the different types of sulfur species present in the catalyst may be detected. Figure 3 shows the TPR-S patterns of the different samples. Here one can observe the presence of two main peaks, one between 373 and 573 K and another between 573 and 973 K. According to Moulijn (11, 12), for Mo and W catalysts supported on alumina, the H_2S evolved in the temperature region 300–550 K can be ascribed to the reduction of sulfur species (Sx), chemisorbed on coordinately unsaturated (cus) edge/corner sites, responsible for the HDS catalytic activity. The peak between 573 and 973 K has been associated also by Moulijn (12) with the recombination of –SH groups and reaction of –SH groups with hydrogen. At higher temperatures ($T > 973$ K), the observed H_2S evolution is related to the reduction of bulk MoS_2 species. In line with the above, the H_2S evolution peaks in these three regions are associated to hydrogen consumption peaks in the TCD signal (not shown). However, the observation of a hydrogen consumption peak at temperatures higher than 973 K without H_2S evolution in the Al_2O_3–TiO_2 support reveals, in agreement with our previous results (6), the reduction of bulk TiO_2.

The TPR-S experiments not only give information on the amount of adsorbed sulfur, but they also give an indication of the ability of the catalysts to hydrogenate the adsorbed sulfur, by observation of the shifts in the temperature of the peak maximum of the Sx hydrogenation. This ability of sulfur hydrogenation is equivalent to the ability of creating sulfur vacancies and, therefore, must be related to HDS

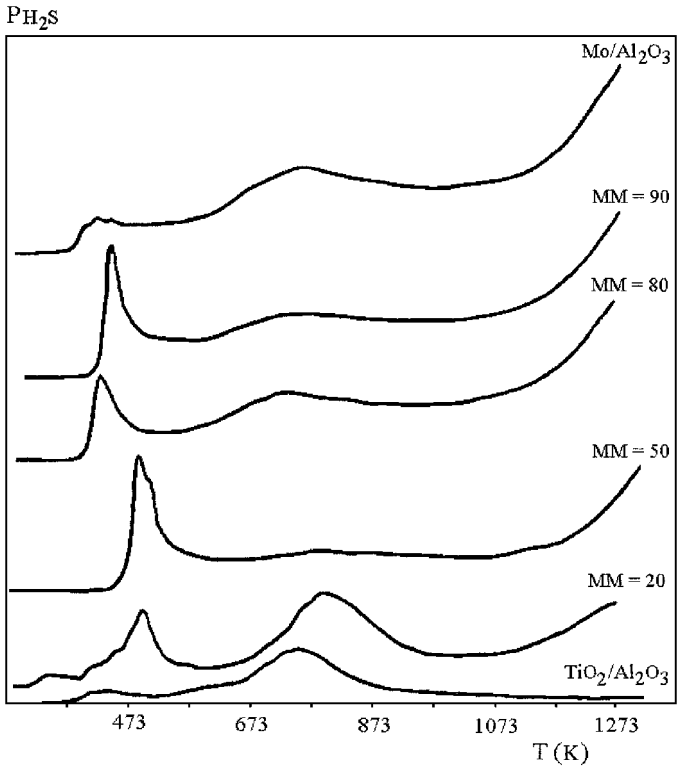

FIG. 3. TPR-S patterns of mechanical mixtures (UV signal).

activity. In fact, a plot of our HDS activity result versus the temperature of the Sx hydrogenation peak maximum (300–550 K), shows an almost linear correlation and indicates that the higher the peak temperature the lower the HDS activity.

A quantitative analysis of the H_2S UV signal in the region 300–550 K of the TPR-S patterns allows us to estimate (12) the number of sulfur vacancies created in the edge/corner sites of the MoS_2 crystallites. The results from this calculation are presented in Table 1, where the estimated amount of H_2S evolved per Mo atom (P_{H_2S}/Mo) is shown. Since this amount of H_2S was calculated from the TPR-S peak

TABLE 1

Catalysts Mechanical Mixtures and Results of TPR-S

Mechanical mixtures (MM)	R_{Mo} (Mo/Ti + Mo)	Mo_t	P_{H_2S}	P_{H_2S}/Mo_t
00	0.000	0.0	1.55	—
20	0.132	27.6	5.70	0.206
50	0.378	79.1	6.11	0.077
80	0.708	148.1	5.35	0.036
90	0.844	176.6	6.28	0.035
100	1.000	209.2	3.76	0.018

Note. Mo_t, total Mo in the catalysts (μ mol); P_{H_2S}, H_2S evolution in temperature region 300–550 K (μ mol).

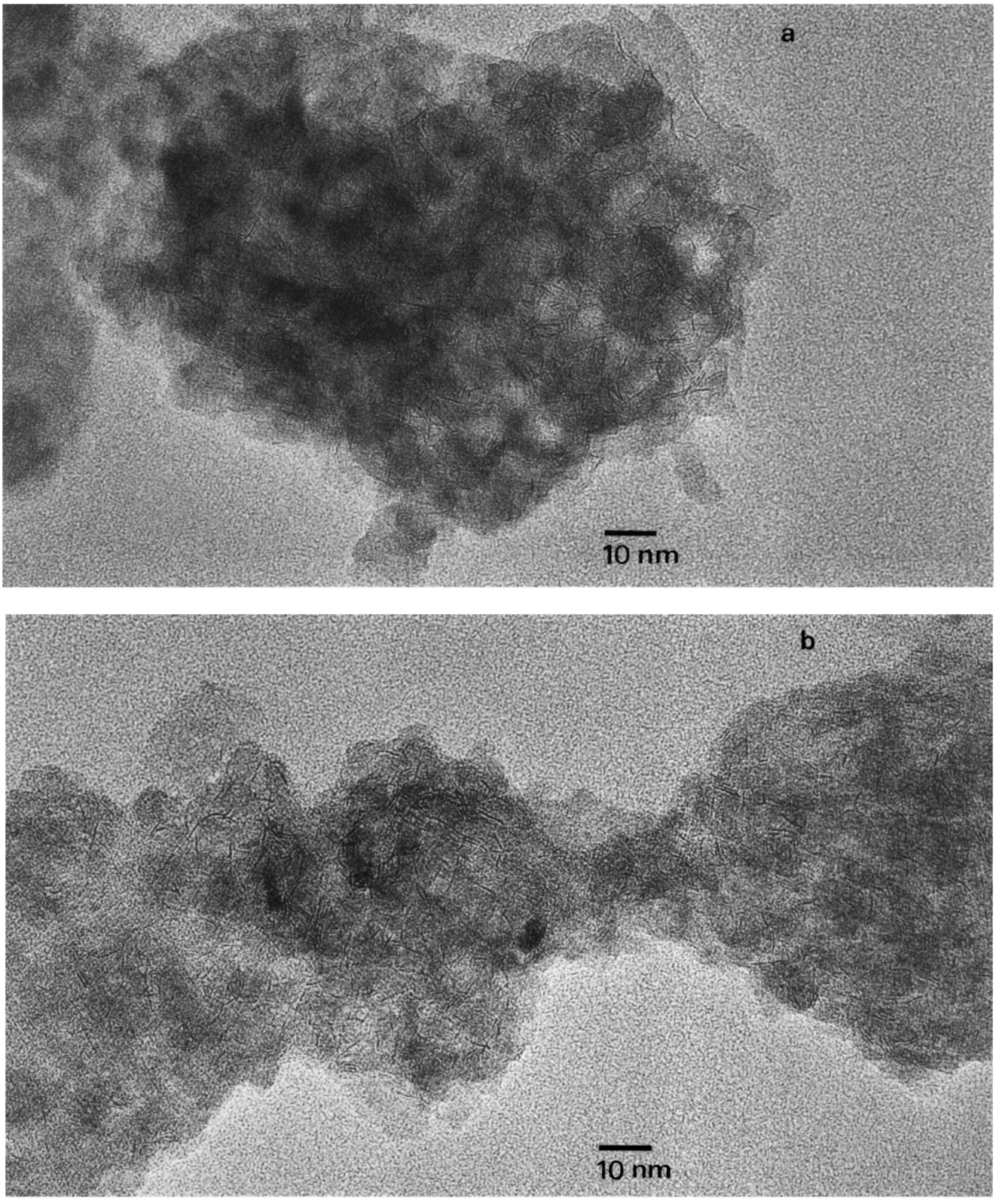

FIG. 4. Micrographs of sulfided Mo/Al_2O_3, (a) before reaction and (b) after reaction.

at 300–550 K, it is equivalent to the sulfur vacancies created in the catalyst. From these results it is clear that not all the Mo atoms present in the MoS_2 crystallites are capable of forming sulfur vacancies at temperatures in the range of reaction conditions, in good agreement with the general belief that it is only the edge/corner Mo sites which are active in HDS. The S/Mo ratio in the Mo/Al_2O_3 catalyst used here before TPR-S was 1.47. This result is in line with the results from Okamoto (13) who found that in Mo/Al_2O_3 catalysts, after thiophene HDS reaction, the S/Mo ratio fluctuates between 1.40 and 1.79 according to Mo loading (2.4 to 23.1 wt% MoO_3). Assuming that all the Mo is sulfided, the difference between these S/Mo ratios with the theoretical value of 2 in MoS_2 would be an estimate of the amount of nonstoichiometric sulfur present in Mo/Al_2O_3 catalysts after reaction.

Since it is widely accepted that Mo edge/corner atoms in the MoS_2 crystallites are the active sites in HDS reactions, and that it is in these sites where the sulfur vacancies are mainly created during reaction, it would also be useful to estimate their number in the sulfided catalysts to have an idea of the number of vacancies, created under TPRS conditions, per Mo atom in edge/corner positions. To this end, HREM micrographs of the sulfided Mo/Al_2O_3 catalyst were taken to estimate the average size and stacking of the MoS_2 crystallites. Figure 4 shows typical micrographs of the Mo/alumina catalyst in which it is possible to observe the well-known layered structures of MoS_2 crystallites, with interplanar distances of about 6.1 Å. Statistics over more than 500 crystallites in the Mo/Al_2O_3 catalyst allowed the estimation of their average length (L_{av}) and number of layers (N_{av}), i.e., $L_{av} = 40$ Å and $N_{av} = 2$. In apparent contrast with previous reports, the HREM micrographs of the sulfided catalysts show that, for our Mo/Al_2O_3 catalysts, there is not a great difference in the size and number of layers of the MoS_2 crystallites observed before and after the reaction, for reactions times of 18 h (see Fig. 4). This is probably due to the short time span of the reaction test and to the Mo loading of our catalysts. From the above results, and using the geometrical model proposed by Kaztelan (14), which assumes, due to stability considerations, a regular hexagonal geometry for the MoS_2 crystallites, it is possible to estimate the number of edge/corner Mo atoms per MoS_2 crystallite and per MoS_2 layer in each average-sized crystallite. Also, since we know the total amount of Mo in the catalyst and considering, based on previous studies (15), that all the Mo present was sulfided, we can estimate the total number of edge/corner Mo atoms present in the catalyst. Figure 5 shows the features of the geometrical model and the relationships used to estimate from the HREM measurements, the total number of Mo atoms (Mo_t), the Mo in edges (Mo_e), and the Mo in corners (Mo_c) in the MoS_2 crystallite. Since in all the TPR-S experiments 0.25 g of catalyst were used, it is possible to calculate the total number of MoS_2 crystallites in each experiment and therefore, the total number of each type of molybdenum (edge, corner, etc.) present in each mechanical mixture. The results from this calculation are presented in Table 2, where the $P_{H_2S}/(Mo_e + Mo_c)$ ratio is also reported, which gives an indication of the average number of sulfur vacancies created per Mo atom present in edge+corner sites. The results show that the number of sulfur vacancies per Mo atom in edge/corner positions increase from 0.058 in the Mo/alumina sample to 0.662 in the mechanical mixture catalyst sample with an atomic ratio $R_{Mo} = 0.132$. Clearly, the value of 0.662 is the average number of vacancies per Mo atom in edge/corner positions. This result gives a clear indication that although more vacancies are formed in the Mo atoms when titanium is present in the catalyst, not all the edge/corner Mo atoms present in the MoS_2 crystallites are capable of forming vacancies under the conditions of our experiment, since it is well known that the HDS and hydrogenation active sites have one and two or three sulfur vacancies, respectively. In any case, the results point to the existence of Mo atoms with a low number of vacancies as the active sites in HDS.

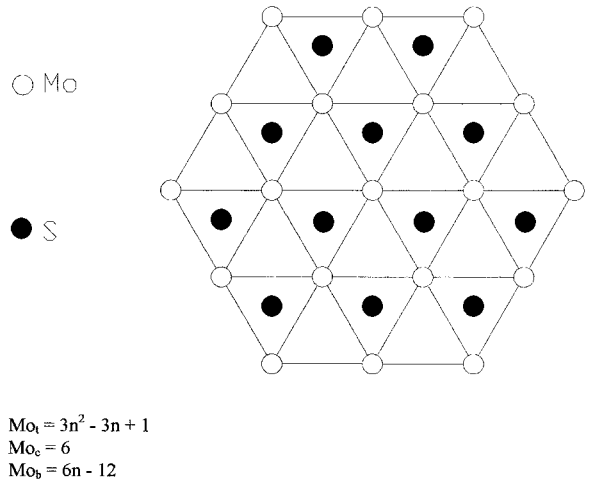

FIG. 5. Features of MoS_2 geometrical model.

TABLE 2

Results of Geometrical Model and Number of Sulfur Vacancies

R_{Mo}	NC	Mo_e	Mo_c	Mo(e + c)	P_{H_2S}/Mo(e + c)
0.132	0.81	4.21	0.97	5.18	0.662
0.378	2.31	12.05	2.77	14.82	0.248
0.708	4.32	22.57	5.18	27.76	0.116
0.844	5.16	26.89	6.18	33.08	0.114
1.000	6.11	31.92	7.34	39.26	0.058

Note. $R_{Mo} = (Mo/Ti + Mo)$ atomic ratio; NC, number of crystallites ($\times 10^{-17}$); Mo_e, Mo in edges (Mo atoms $\times 10^{-18}$); Mo_c, Mo in corners (Mo atoms $\times 10^{-18}$); P_{H_2S}, H_2S evolution in temperature region 300–550 K, equivalent to the sulfur vacancies.

The product distribution results of the different catalyst compositions show that the yield of the hydrogenated product, butane, expressed as (butane/(butane + butenes)), reaches a maximum at the same composition as for thiophene HDS (80% Mo/Al_2O_3–20% TiO_2/Al_2O_3). These results indicate that the hydrogenating function of the catalyst is also promoted by the presence of TiO_2. The same maximum for thiophene HDS and hydrogenation of butenes to butane has been also reported for $CoMo/Al_2O_3$ catalysts modified with boron (16), where it was suggested that butene hydrogenation took place on a site similar to HDS, i.e., a single vacancy site. It has been previously suggested that small chain olefins can be hydrogenated over a single sulfur vacancy and do not require two or three, as would be required for the hydrogenation of aromatics (17).

It is also interesting that the apparent activation energies for the thiophene transformation, calculated for the different mechanical mixtures, decreases from 23 to 18 kcal/mol as the content of TiO_2/Al_2O_3 in the mechanical mixture diminishes. We have interpreted this result by considering that although the thiophene HDS reaction on partly sulfided TiO_2/Al_2O_3 is more difficult than on MoS_2/Al_2O_3, the presence of the former in the mechanical mixture increases the number of potentially active sites in the latter, as the TPR-S results indicate.

Although to this point we have been able to relate the beneficial effect of the presence of TiO_2 in Mo/Al_2O_3 catalysts to the formation of a greater number of sulfur vacancies, the fact that TiO_2 is a semiconductor must also have some effect on the electronic and redox properties of the catalyst. To inquire on this, analysis of the DRS electronic spectra of the oxided and sulfided state of Al_2O_3, TiO_2, Mo/Al_2O_3, TiO_2/Al_2O_3, and a mechanical mixture (MM = 50) samples was performed.

It is well known that alumina does not give rise to any absorption in the wavelength region 200–2200 nm of the spectrum, except for the bands located near 1400 and 1900 nm, which are vibrational overtone transitions involving the surface hydroxy groups. The lack of any electronic transition in this region is due to the close shell structure of Al and oxide ions, and to the electronic structure of this solid that is an insulator and is characterized by an energy gap between the O2*p* valence band and the Al3*s*,3*p* conduction band of 7 eV. The DRS spectrum of alumina (not shown) does not change under sulfidation, showing that this material cannot be either reduced or sulfided under the experimental sulfidation, conditions used here.

In Fig. 6 the UV–vis DRS spectra the Mo/Al_2O_3 catalyst in its oxided and sulfided states are compared. The spectrum of the Mo/Al_2O_3 sample in its oxidic state shows, in addition to the above cited vibrational overtone bands, a strong absorption band with a maximum at 240 nm with an absorption onset just near 550 nm. This absorption has the typical shape of a band, and is assigned to level-to-level

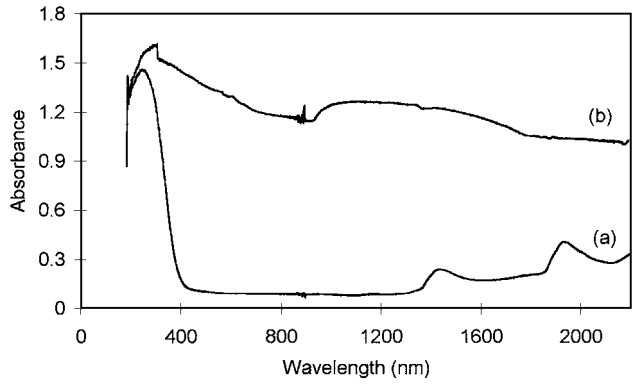

FIG. 6. DRS spectra of Mo/Al_2O_3 catalyst in (a) oxided and (b) sulfided state.

electronic transition of nearly isolated Mo species. It is typically found in Mo(VI) oxo-species and can be assigned to the O2$p \rightarrow$ Mo4*d* charge transfer transition. The spectrum of this sample changes drastically after sulfidation and in this case we see again a maximum, apparently shifted now near 300 nm, a region of strong absorption between 900 to near 1400 nm, and a tail in the region 1400–1700 nm. Additionally, an almost continuous absorption is found in the overall spectrum. This very evident modification of the DRS spectrum of the Mo/Al_2O_3 sample after sulfidation implies that reduction or sulfidation of the sample took place. Indeed, sulfidation of the sample was confirmed by HREM (see Fig. 4).

According to previous work, the UV spectrum of the MoS_2 crystallites is characterized by a very evident edge at 800–1000 nm (18), associated, according to energy band calculations, to the electron transition from the highest occupied Mo3*d* (z^2) orbital to the lowest unoccupied Mo3*d* (x^2-y^2, xy) orbital (19). The energy difference between these levels is 1.2 eV. However, by decreasing the MoS_2 crystal size, the absorption region extends with a tail toward lower energies (higher wavelengths), likely due to the absorption of surface defects (18). In the case of colloidal MoS_2 particles, a suppression of the absorbance peaks in the band edge exciton region between 1.2 and 1.7 eV (580–730 nm) was observed and increased absorbance was found below 1.7 eV (730 nm) (20). Therefore, the absorption we find in the region 900–1700 nm for the sulfided Mo/Al_2O_3 sample is apparently the extreme result of the MoS_2 particle size decrease and surface defects increase. Indeed, our HREM observations indicate we are dealing with very small crystallites on the order of 40 Å. In this case, the absorption maximum that we observe at the lower wavelength region, below 900 nm, is likely associated to unsulfided and/or unreduced Mo oxidic species, while the almost continuous absorption would be associated to the reduced and/or sulfided Mo species dispersed on the alumina surface.

The DRS spectrum of TiO_2, not shown, is characterized by an absorption edge the high wavelength limit of which is detected at 330 nm with an absorption onset at 400 nm. This absorption is typically found for TiO_2, anatase (4, 21), and is assigned to the O2*p*–Ti3*d* charge transfer transition, corresponding to the transfer of electrons from the valence band to the conduction band. This behavior characterizes TiO_2, anatase, as a semiconductor solid with an energy gap of near 3.0 eV.

Figure 7 compares the UV–vis spectra of the TiO_2/Al_2O_3 in its oxidic and sulfided state. The spectrum of the oxidic TiO_2/Al_2O_3 is characterized by an adsorption edge with a lower limit near 370 nm and the onset at 600 nm. This edge is shifted up with respect to TiO_2, anatase, and this can be associated to the morphology of the titania particles that have been impregnated on the surface of alumina. After sulfidation, the absorption base line is definitely shifted upward in the region below 1300 nm with no evident maximum. This absorption seems to increase as the wavelength decreases down to near 600 nm, where the onset of the titania absorption edge is found. However, this edge is not so well defined, with perhaps a component in the region 400–500 nm. The modification of the spectrum of the sulfided sample with respect to the unsulfided one shows that sulfidation and/or reduction of the TiO_2/Al_2O_3 sample occurs to some extent. The observed absorption change can be associated to the formation of TiS_2, which is a narrow gap semiconductor (22–24), the energy gap of which has been measured to be as low as 0.2 eV (23). In fact, it has been reported that TiS_2 takes a metal character by reduction to $Ti_{1+x}S_2$ (25), and that TiO_2 becomes a conductor under reduction (26), although partial reduction of TiO_2 only results in the formation of electrons that can be trapped (at least at low temperature) forming Ti^{3+} cations detectable by ESR (27). In both cases the conduction band arises from the Ti3*d* levels that become partly occupied as a result of the Ti(IV) reduction. Localized electrons forming Ti^{3+} cations in the TiO_2 particles can be responsible for the additional absorbance observed at 400–500 nm in the TiO_2/Al_2O_3 sulfided sample.

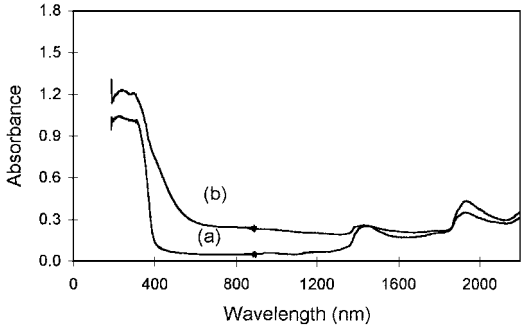

FIG. 7. DRS spectra of TiO_2/Al_2O_3 sample in (a) oxided and (b) sulfided state.

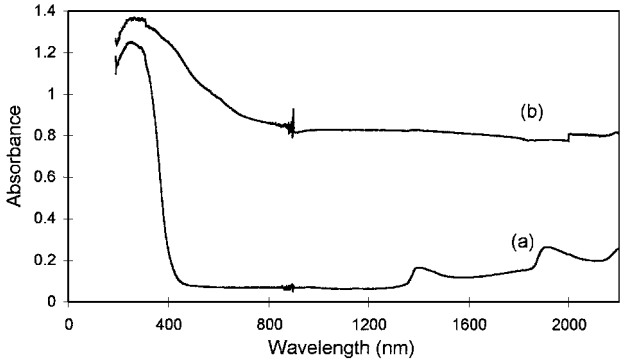

FIG. 8. DRS spectra of Mo/Al_2O_3–TiO_2/Al_2O_3 mechanical mixture (MM = 50). (a) Oxided and (b) sulfided state.

In Fig. 8, the UV–vis DRS spectra of the mechanical mixture sample (MM = 50) in their oxided and sulfided forms are compared. The spectrum of the oxided sample shows also an edge; however, in this case the higher wavelength limit of this edge is near 260 nm and the absorption onset is near 600 nm. The absorption observed in the region 220–400 nm is associated with a band-to band transition. In this case this absorption must also contain both the O2$p \rightarrow$ Ti3*d* electron transition, and the O2$p \rightarrow$ Mo4*d* transitions of the molybdate or molybdenyl surface species. The slight shift of the absorption edge of the mechanical mixture to lower energies with respect to that of TiO_2/Al_2O_3 suggests that the Mo4*d* levels are either located in the gap just below the lower limit of the TiO_2 conduction band, or that they participate to the conduction band and cause its shift to lower energies. This observation is quite important since it indicates that in this case the molybdenum phase and the support are electrically connected through the conduction band and can form a redox pair.

The UV–vis spectrum of the sulfided mechanical mixture sample is very different from the unsulfided sample confirming that sulfidation and/or reduction of the sample has taken place. Its shows the appearance of continuous absorption in the overall region and the permanence of the TiO_2 characteristic absorption at 200–400 nm is also observed. The spectrum is not very different from the one observed in the case of the sulfided Mo/Al_2O_3 sample, although here we note a weaker absorption in the region assigned to MoS_2 particles (950–1400 nm), probably due in part to the dilution effect of the TiO_2/Al_2O_3 incorporated in the mechanical mixture (MM = 50). Also, the slope at the lower wavelength region below 900 nm is higher indicating a smaller population of unsulfided and/or unreduced Mo oxidic species.

The above results show that alumina, titania, and titania/alumina can behave differently as supports for MoS_2 particles. Alumina is an insulator and cannot be either oxidized or reduced by sulfidation treatments. In other words, no electronic interaction can occur between the unoccupied

Al3*s* and 3*p* orbitals and the *d* orbitals of Mo, either in the oxidized or in the reduced and sulfided states. In fact, the Al empty orbitals are too far in energy to exchange electrons with those of molybdenum. In contrast, for titania-containing catalysts, the Ti3*d* levels and the titania conduction band that arises from them are located at much lower energy so that they are closer to the Mo4*d* orbitals. For the oxidized samples it appears that the Mo4*d* orbitals lie in the titania conduction band or just below it. This clearly makes the MoO_3/TiO_2 powders a semiconductor solid where the different Mo oxide centers are in electronic contact with one another and with the Ti cations through the conduction band. In contrast, in the alumina-supported catalysts, the Mo oxide and sulfide centers of different particles are electronically isolated from each other and from the support.

It seems clear now that in the case of titania-supported hydrotreating catalysts, after sulfidation and in reaction conditions, where the catalyst is in the presence of a high hydrogen partial pressure, titania can be reduced and sulfided in part. Moreover, under these conditions the reduced titanium oxide and titanium sulfide species, the latter having narrow gap semiconductor properties, will have nearly metal conductivities.

According to previous studies (7, 8) the reduced Ti^{3+} species are easily formed by reduction of Ti^{4+} under hydrogen atmosphere and temperature. These Ti^{3+} ions are preferably located at the surface of TiO_2 and can be easily reoxidized. That is, the 3*d* electron "in excess" in each Ti^{3+} has the tendency to be transferred. In the case of double oxides (i.e., TiO_2–Al_2O_3) the Ti^{3+} ions are stabilized and, in this case, only the Ti^{3+} ions which do not form part of the mixed oxide can be reoxidized easily (25). This means that in the case of double oxide supports such as TiO_2–Al_2O_3, the reduction Ti^{4+} to Ti^{3+} and its reoxidation will only occur easily in the titanium-rich side of the double oxide formulation where some segregation of TiO_2 particles occurs.

In the case of the sulfided catalysts, the supported molybdenum sulfide active phase has also semiconductor properties. In this case, according to the calculations of Harris and Chianelli (28, 29), the empty orbital of Mo in MoS_2 should lie very near the *d* orbital of Ti in TiS_2. This means that under reaction conditions, where a high hydrogen partial pressure exists, partial reduction of TiO_2 and/or TiS_2 surface layers likely occurs and under these conditions electrons from Ti^{3+} species can easily be injected to the Mo3*d* conduction band. This, according to Harris and Chianelli (29), is the requirement for MoS_2 promotion in HDS catalysts. In fact, low valent Mo species were found in an XPS study made by Shimada (30) on Mo/TiO_2 sample. It was suggested that these low valent Mo species were produced by charge transfer from Ti^{3+} ions in the TiO_2 support.

It becomes clear now, based on the above discussion, that the role of titania in HDS catalysts is not only that of a conventional support but, more important, that of an electronic promoter of the molybdenum sulfide phase. Since our catalysts were constituted by sulfided mechanical mixtures of MoO_3/Al_2O_3 and TiO_2/Al_2O_3 powders, it appears due to the synergy effect observed that the above promotion can also occur when there are only a few physical contacts between the particles, since electronic contact is maintained through the conduction band. According to the catalytic activity results, the titanium phases formed under HDS reaction conditions seem to be able to activate hydrogen and perform, although to a small extent, the hydrogenolysis of the carbon–sulfur bond. The above observations and those made previously on the behavior of Al_2O_3–TiO_2 mixed oxide supports of Mo and W phases in hydrodesulfurization catalysts (6, 9) explain clearly why it is only in the titanium-rich Al_2O_3–TiO_2 supports, when the surface contains titania particles, which under reaction conditions can participate in a redox process, that a significant increase in the HDS catalyst activity is observed.

Finally, the fact that unpromoted Mo/TiO_2 catalysts are more active than Mo/Al_2O_3 ones, together with the observation that the synergy effect produced by the Co promoter in CoMo HDS catalysts is greater in $CoMo/Al_2O_3$ than in $CoMo/TiO_2$, although the $CoMo/TiO_2$ catalysts are in overall more active (1), indicates that the observed TiO_2 electronic promotion of the Mo phases is similar in nature to that of Co. Furthermore, quite possibly, there is a limit to this type of promotion since the observed Co promotion effect in $CoMo/Al_2O_3$ catalysts is 2.3 times greater than in $CoMo/TiO_2$ catalysts, where the Mo is already partially promoted by the presence of TiO_2.

All the above results are also in good agreement with the recently proposed Bond Energy Model (31) since the injection of electrons from Ti to Mo will decrease the Mo–S bond energy producing a more active catalyst.

CONCLUSIONS

From the above results it is possible to conclude that:

1. The presence of titanium oxide in MoS_2/Al_2O_3 HDS catalysts induces a synergy effect which enhances the catalyst activity. This effect seems to be related to the presence of Ti^{3+} species, which are formed under reaction conditions and act as a promoter to the MoS_2 phase. Also, apparently, for this effect to be present it is only necessary for the titanium phase to have a few intimate physical contact points with the MoS_2 phase, since electronic contact is maintained through the conduction band of the solids.

2. Not all the edge/corner Mo atoms in MoS_2 crystallites are active in HDS or hydrogenation reactions. It appears, in line with previously reported results, that to perform HDS, the active site requires a low number of sulfur vacancies per Mo atom.

ACKNOWLEDGMENTS

We acknowledge the financial support from PEMEX-Refinación, the IMP-FIES program, to CONACyT(México) and the CNR (Italy). We also are grateful to Mr. Ivan Puente for the HREM micrographs.

REFERENCES

1. Ramirez, J., Fuentes, S., Diaz, G., Vrinat, M., Breysse, M., and Lacroix, M., *Appl. Catal.* **52**, 211–224 (1989).
2. Okamoto, Y., Maezawa, A., and Imanaka, T., *J. Catal.* **120**, 29–45 (1989).
3. Luck, F., *Bull. Soc. Chim. Belg.* **108**, 781–800 (1991).
4. Ramirez, J., Ruiz-Ramirez, L., Cedeño, L., Harle, V., Vrinat, M., and Breysse, M., *Appl. Catal. A* **93**, 163–180 (1993).
5. Ozaki, H., *Catal. Surveys Jpn.* **1**, 143–156 (1997).
6. Ramirez, J., and Gutierrez, A., *J. Catal.* **170**, 108–122 (1997).
7. Zhaobin, W., Qin, X., Xiexian, G., Sham, E., Grange, P., and Delmon, B., *Appl. Catal.* **63**, 305–317 (1990).
8. Zhaobin, W., Qin, X., Xiexian, G., Grange, P., and Delmon, B., *Appl. Catal.* **75**, 179–191 (1991).
9. Damyanova, S., Spojakina, A., and Jiratova, K., *Appl. Catal. A* **125**, 257–269 (1995).
10. Gutierrez, A., Trombetta, M., Busca, G., and Ramirez, J., *Microporous Mater.* **12**, 79–91 (1997).
11. Scheffer, B., Dekker, N., Mangnus, P., and Moulijn, J., *J. Catal.* **121**, 31–46 (1990).
12. Mangnus, P., Bos, A., and Moulijn, J., *J. Catal.* **146**, 437–448 (1994).
13. Okamoto, Y., Maezawa, A., and Imanaka, T., *J. Catal.* **120**, 29–45 (1989).
14. Kaztelan, S., Toulhoat, H., Grimblot, J., and Bonnelle, J., *Appl. Catal.* **13**, 127–159 (1984).
15. Zhaobin, W., Qin, X., and Xiong, G., *Catal. Lett.* **15**, 255–267 (1992).
16. Ramirez, J., Castillo, P., Cedeño, L., Cuevas, R., Castillo, M., Palacios, J. M., and Lopez-Agudo, A., *Appl. Catal. A: General* **132**, 317–334 (1995).
17. Anderson, J., and Boudart, M., "Catalysis Science and Technology," Vol. 11, Springer Verlag, 1996.
18. Roxlo, C. B., Daage, M., Ruppert, A. F., and Chianelli, R. R., *J. Catal.* **100**, 176 (1986).
19. Keyong, Ae. Yee., and Hughbanks, T., *Inorg. Chem.* **30**, 2321 (1991).
20. Wagoner, G. A., Persons, P. D., and Ruppert, R. A., *Mater. Res. Soc. Symp. Proc.* **283**, 909 (1993).
21. Bevan, H., Dawes, S. V., and Ford, R. A., *Spectrochim Acta* **13**, 43 (1958).
22. Wilson, S. A., *Phys. Status Solidi B* **86**, 11 (1978).
23. Brauer, H. E., Starnberg, H. I., Holleboom, L. J., and Hughes, H. P., *Surf. Sci.* **419**, 331–333 (1995).
24. Faba, M. G., Gonbeam, D., and Pfister-Guillouzo, G., *J. Electron. Spectrosc. Relat. Phenom.* **73**, 65 (1995).
25. Molenda, J., *J. Therm. Anal.* **38**, 2163 (1992).
26. Ookubo, A., Kanezaki, E., and Ooi, K., *Langmuir* **6**, 206–209 (1990).
27. Che, M., Thesis, Lyon, Univ. Claude Bernard, France, 1968.
28. Harris, S., and Chianelli, R. R., *J. Catal.* **86**, 400 (1984).
29. Harris, S., and Chianelli, R. R., *J. Catal.* **98**, 17 (1986).
30. Shimada, H., Sato, T., Yoshimura, Y., Hiraishi, J., and Nishijima, A., *J. Catal.* **110**, 275–284 (1988).
31. Byskov, L. S., Norskov, J. K., Calusen, B. S., and Topsoe, H., "Preprints Symposia Recent Advances in Heteroatom Removal," Vol. 43, pp. 12–14, 1988. [See references therein]